Asian Journal of Chemistry; Vol. 36, No. 2 (2024), 317-324

ASIAN JOURNAL OF CHEMISTRY

https://doi.org/10.14233/ajchem.2024.30581

An Efficient Adsorption of Safranin O Dye on Ascorbic Acid Coated Nanoparticles: Thermodynamics, Kinetics and Isotherm Studies

KEERTI RANI, JAIVEER SINGH, ARTI JANGRA, JAI KUMAR and RAMESH KUMAR*

Department of Chemistry, Kurukshetra University, Kurukshetra-136119, India

*Corresponding author: E-mail: rameshkumarkuk@gmail.com; rameshchemkuk@kuk.ac.in

Received: 28 September 2023; *Accepted*: 3 December 2023; *Published online*: 31 January 2024; AJC-21518

In present work, the chemical co-precipitation method was used to prepare the ascorbic acid coated magnetite nanoparticles (AA-MNPs) which were then applied for the elimination of hazardous dye safranin O from the contaminated water. With the help of XRD peaks and Debye-Scherrer equation, the average size of the ascorbic acid coated nanoparticles was found to be 18 nm. These surface coated nanoparticles were further characterized using FTIR, TGA, FESEM and VSM methods. Thus, formed surface functionalized magnetite nanoparticles (MNPs) were used for the removal of safranin O dye from the contaminated water, using batch adsorption technique by considering dosage of AA-MNPs, dye concentration, pH of solution and temperature. It was found that synthesized AA-MNPs showed the highest dye removal efficacy (more than 97%) when the dye concentration was taken 50 ppm. Different thermodynamic parameters were measured, including ΔG°, ΔH° and ΔS°. Adsorption of safranin O dye on the surface of AA-MNPs was found to be exothermic and spontaneous, according to thermodynamic parameters. The Freundlich model matched the experimental equilibrium data better, implying a heterogeneous multilayer adsorption on nanoparticles surface, according to the isotherm analysis. Moreover, the investigation of kinetic data suggested a pseudo 2nd order rate for the safranin O dye adsorption process. In addition, a comparative investigation has been made for the efficacy of the removal of safranin O dye by ascorbic acid coated magnetic nanoparticles with the adsorbents that have previously been reported.

Keywords: Magnetite nanoparticles, Ascorbic acid, Safranin O, Adsorption, Kinetics.

INTRODUCTION

Nowadays, with the huge growth of many industries, the quality of water has been deteriorated by discharging various toxins such as dyes, heavy metal ions and a variety of other organic pollutants [1]. Specially, dyes are regarded as a source of water pollution as they are frequently used in the production of paint, paper, textiles, food, cosmetics and pigments [2]. As a result of large-scale production and broad use, many dyes have found their way into various water bodies [3]. One of the most well-known cationic dyes is safranin O (SO), which is utilized in pharmacy as a veterinary medicine. Safranin O dye is also used as a flavouring and colouring agent in cuisine. Safranin O is also being used to dye fabrics like cotton, wool, silk as well as leather and paper [4]. Furthermore, due to high water solubility of SO dye, it was found in high concentrations in the wastewater released from various industries [5]. At excess quantities in aquatic environments, this dye was claimed to be poisonous, allergic or carcinogenic [6]. As a result, elimination of dyes from wastewater is a vital requirement for survival of aquatic life and pollutant free water.

Several processes are used to decontaminate wastewater, including the membrane method, adsorption method, biodegradation and chemical oxidation approach [7]. Because of the high efficiency, simplicity and cost effectiveness, the adsorption method for dye removal is frequently used [8]. Nanostructured substances have huge surface-area-to-volume ratio and hence they have extra advantages for effective adsorption process with a variety of good adsorbents. Moreover, nanoparticles are also a good adsorbent for dye removal due to the characteristic structural, optical and magnetic properties. Due to high magnetic saturation, minimal toxicity and biocompatibility, superparamagnetic iron oxide (Fe_3O_4) nanoparticles have emerged as a promising candidate for various applications in modern technologies [9]. Several research groups have reported the decontamination of the wastewater from SO dye

by using various types of adsorbent materials [10-15]. However, SO dye removal efficiency was found less effective with all these reported adsorbent materials. In this investigation, a novel adsorbent material is employed that exhibits exceptional efficacy in eliminating the SO dye from the wastewater. The current effort includes the synthesis of iron oxide nanoparticles with the ascorbic acid coating as a safranin adsorbent material. Various factors impacting SO dye adsorption from aqueous solution such as pH, contact time, initial dye concentration, adsorbent dosage and temperature were investigated. In addition to these, the adsorption isotherm, kinetics and thermodynamics studies were also carried out.

EXPERIMENTAL

All the analytical grade chemicals used in this study *viz.* ferrous sulfate heptahydrate ($FeSO_4 \cdot 7H_2O$, 98%), ferric chloride hexahydrate ($FeCl_3 \cdot 6H_2O$, 98%), ammonium hydroxide solution (25%), safranin O dye and ascorbic acid were procured from SRL (India) with no additional purification.

ABB MB-3000 FTIR spectrometer was used to record the infrared spectra of bare and ascorbic acid coated magnetite nanoparticles. Thermal examination of bare as well as coated nanoparticles was carried out using a Perkin-Elmer STA-6000 thermogravimetric analyzer. A T90 PG Instrument Limited UV-Vis spectrophotometer was used to measure the absorbance studies. The Hitachi SU-8000 field emission scanning electron microscope (FESEM) was used to measure the average size of uncoated and coated nanoparticles. At room temperature, X-ray diffraction (XRD) patterns were recorded using an X-ray source radiation having wavelength of 1.5406 Å. Uncoated and coated magnetic nanoparticles were synthesized using a digital overhead stirrer (2000 rpm).

Synthesis of Fe_3O_4 and AA-Fe_3O_4 nanoparticles: The co-precipitation method was used for preparation of the naked and coated magnetite nanoparticles. A 50 mL ferrous sulphate solution was mixed with 50 mL ferric chloride solution in a 1:2 molar ratio at first. The resulting solution was heated to 85 ºC in an inert gas environment by vigorously swirling it for nearly 0.5 h. A 20 mL of ammonia solution was added to the resultant mixture till pH value raised to 10. A change in colour from brown to black confirmed the formation of Fe_3O_4 nanoparticles [16]. After that 2.6 g ascorbic acid dissolved in water (50 mL) was promptly added to this solution and agitated for additional 1 h. The AA-Fe_3O_4 nanoparticles were separated from the solution using an external magnetic field and washed with deionized water. After drying in a vacuum oven, the surface-modified magnetic nanoparticles were analyzed using XRD, FTIR, FESEM and TGA techniques.

Preparation of safranin O (SO) dye solution: A 50 ppm of stock solution of safranin O dye was prepared. In the visible range, the maximum absorption peak for safranin O was found at 520 nm. The concentration of solution was varied between 10 and 50 ppm. At 520 nm, the absorbance was measured for different concentrations. A standard curve was obtained by plotting the graph of absorbance *versus* safranin O dye concentration at the highest wavelength. A linear plot with a good coefficient of determination ($R^2 = 0.997$) was achieved (Fig. 1).

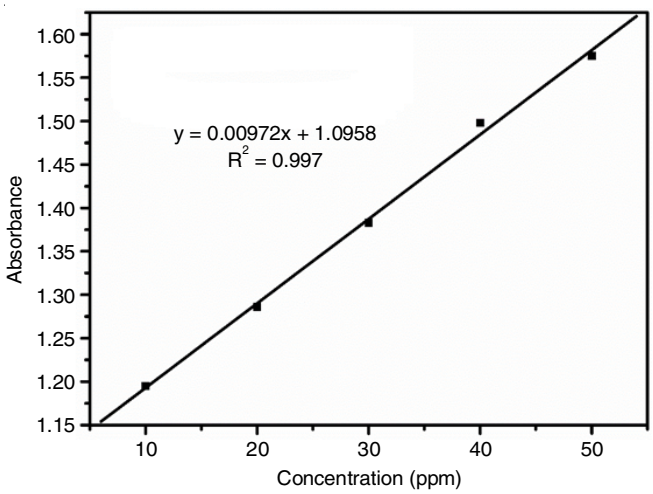

Fig. 1. Standard curve for determination of safranin O dye concentration

Batch adsorption studies: To analyze the efficiency of synthesized ascorbic acid coated magnetite nanoparticles (AA-MNPs) in removing SO dye, a series of batch experiments were conducted. After stirring the dye containing nanoparticles sample for a definite interval of time, aliquots were taken and sonicated for 5 min to conduct the measurements. The studies were carried out by varying the initial SO dye concentrations (10-50 ppm), pH (3-7) and nanoparticles doses (5-30 mg). A 0.1 M HCl and 0.1 M NaOH were used to alter the pH of solution. A UV-vis spectrophotometer was used to examine the supernatant. The removal percentage of SO dye by AA-MNPs was determined by using eqn. 1:

$$R\ (\%) = \frac{C_o - C_e}{C_o} \times 100 \quad (1)$$

where C_o (ppm) = the initial concentration of dye; C_e (ppm) = the SO dye concentration at equilibrium state. The capacity of adsorption of the AA-MNPs was obtained by using eqn. 2:

$$q_t (mg/g) = \frac{(C_o - C_t)V}{m} \quad (2)$$

where q_t = adsorption capacity of AA-MNPs at a time interval t in mg/g; C_o (ppm) and C_t (ppm) are the initial SO dye concentration and SO dye concentration at time interval t, sequentially. V = volume of SO dye used (L) and m = mass of AA-MNPs used (g) [17-20].

RESULTS AND DISCUSSION

Characterization of Fe_3O_4 and AA-Fe_3O_4 nanoparticles

Infrared studies: The presence of an ascorbic acid (AA) coating on the surface of a magnetite nanoparticle is confirmed by comparing the pure ascorbic acid, Fe_3O_4 nanoparticles and AA coated Fe_3O_4 nanoparticles IR spectra (Fig. 2). In the IR spectrum of pure ascorbic acid, the peaks at ~3526-3215 cm^{-1} may be assigned to the stretching vibrations of -OH groups of the ascorbic acid. The stretching vibrations of carbonyl group of five-membered lactone ring corresponds to a distinctive absorption peak at 1755 cm^{-1} in the infrared spectrum of pure ascorbic acid. This low value of carbonyl group of five membered

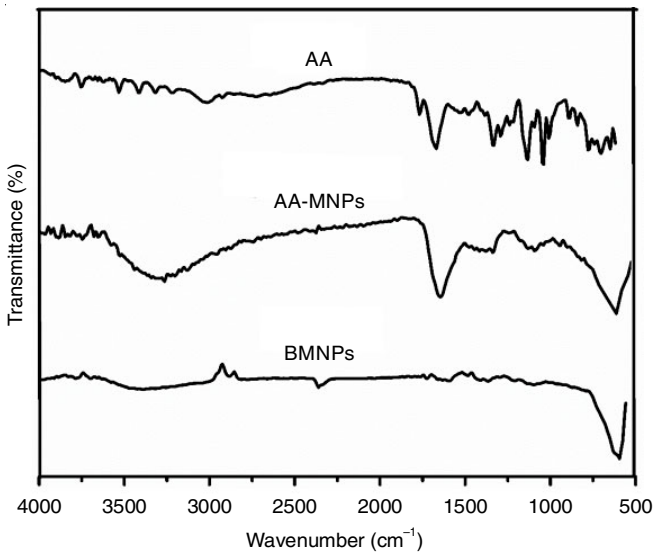

Fig. 2. FTIR spectra of bare magnetic nanoparticles (BMNPs), ascorbic acid coated magnetic nanoparticles (AA-MNPs) and pure ascorbic acid (AA)

lactone may be justified on account of presence of double bond between α and β carbon atoms, which contribute to conjugation. Also, a band at 1656 cm^{-1} in the IR spectrum of ascorbic acid may be due to C=C stretching vibrations. During surface functionalization of Fe_3O_4 nanoparticles with ascorbic acid, in aqueous solution ascorbic acid get oxidized. In the IR spectrum of AA-Fe_3O_4 nanoparticles, the disappearance of the carbonyl band and appearance of a new adsorption band at 1620 cm^{-1} after coating showed that the O atom of carbonyl group of lactone ring has coordinated to the $Fe^{2+}$and Fe^{3+} of iron oxide nanoparticles. The significant difference in the locations of distinct bands of coated and pure ascorbic acid provides the proof for the coating of ascorbic acid on the surface of Fe_3O_4 NPs. Furthermore, a common peak around 600 cm^{-1} is observed in the infrared spectra of bare Fe_3O_4 and AA-Fe_3O_4 nanoparticles, which is due to the Fe-O vibrations.

X-ray diffraction (XRD) studies: The crystallite sizes of the prepared nanoparticles were investigated using an X-ray diffractometer. The XRD patterns of Fe_3O_4 and AA-Fe_3O_4 nanoparticles were recorded (Fig. 3). The Debye-Scherrer equation was used to calculate the mean crystallite size of the nanoparticles:

$$d = \frac{0.9\lambda}{\beta\cos\theta} \quad (3)$$

where d is the mean crystallite size, θ is the Bragg angle, λ is the X-ray source wavelength in nm and β represents the full width at half maximum (FWHM) of the most intense peak [21,22]. Using the Scherrer's equation and FWHM of the maximum intense peak, the average crystallite sizes for bare Fe_3O_4 and ascorbic acid coated Fe_3O_4 nanoparticles were found to be 11.79 and 17.11 nm, respectively. The crystallite size of Fe_3O_4 and ascorbic acid coated magnetite nanoparticles obtained by the Debye-Scherrer equation was found to be close to the FESEM analysis results. Due to this, the size (in nm) of bare and coated MNPs was confirmed by both XRD studies and FESEM studies simultaneously.

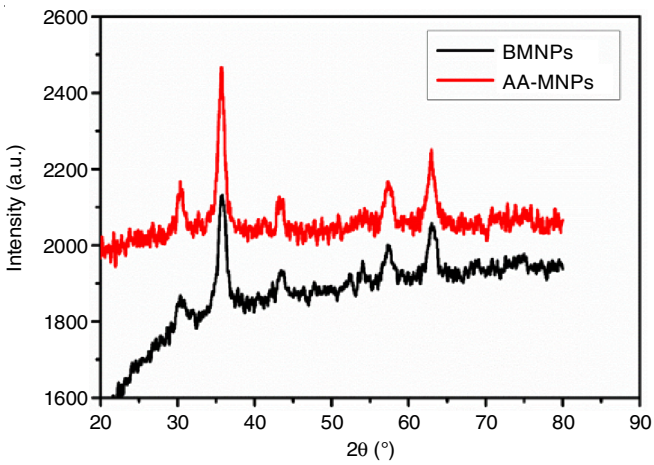

Fig. 3. XRD patterns of bare magnetic nanoparticles (BMNPs) and ascorbic acid coated magnetic nanoparticles (AA-MNPs)

FESEM studies: The surface morphology of uncoated Fe_3O_4 and ascorbic acid coated Fe_3O_4 (AA-Fe_3O_4) nanoparticles were studied using FESEM technique (Fig. 4). The average particle size of bare nanoparticles was found to be 15.91 nm from the FESEM image of the nanoparticles. Whereas, the mean size of the coated nanoparticles was found to be 21.13 nm from the FESEM studies. The increase in size of ascorbic acid coated nanoparticles confirmed that surface of Fe_3O_4 nanoparticles were coated by ascorbic acid.

Thermal studies: The TGA curves of bare and ascorbic acid coated magnetite nanoparticles displayed several degradation stages of the same at different temperatures (Fig. 5). At first stage, both uncoated and coated sample showed a weight loss at ~100 ºC, which may be due to the removal of the adsorbed moisture from these samples. Above 100 ºC, weight loss of around 25% was reflected by TGA curve of ascorbic acid coated magnetite nanoparticles, which may be justified on the basis of degradation of coating *i.e.* ascorbic acid from the surface of Fe_3O_4 nanoparticles. These observations of thermal studies also led to the conclusion of successful coating of ascorbic acid on surface of magnetite nanoparticles.

Vibrating sample magnetometer (VSM) study: Magnetic properties of synthesized magnetite nanoparticles were carried out using VSM study. The magnetic hysteresis curves of Fe_3O_4 nanoparticles and AA-Fe_3O_4 nanoparticles were obtained at 300 K (Fig. 6). The superparamagnetic behaviour of both Fe_3O_4 nanoparticles and AA-Fe_3O_4 nanoparticles was confirmed by hysteresis loops. At 300 K, Fe_3O_4 nanoparticles exhibited a saturation magnetization (M_s) value of 59.76 emu/g while AA-Fe_3O_4 NPs showed an M_s of 44.85 emu/g. These results are the reflection of successful coating of non-magnetic material on surface of magnetite nanoparticles due to which M_s value of AA-Fe_3O_4 nanoparticles was found to be low as compared to M_s value of bare Fe_3O_4 nanoparticles. The decrease in the value of M_s was due to an electron exchange between the Fe atomic surface and the coating material [23]. However, the results showed that after coating the Fe_3O_4 nanoparticles with ascorbic acid, there was no significant drop in M_s for the nanoparticles, showing that the coating had no effect on the superparamagnetic behaviour of Fe_3O_4 nanoparticles.

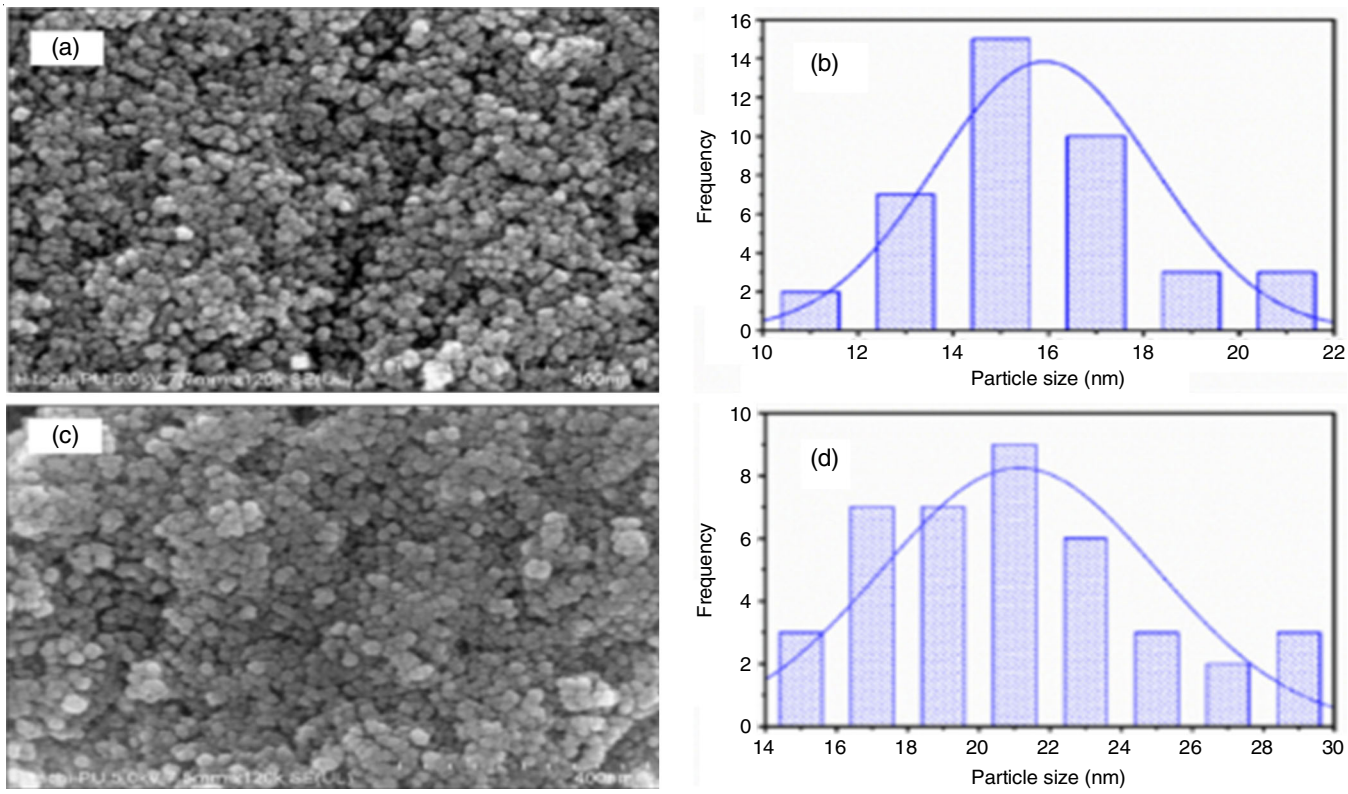

Fig. 4. (a,b) FESEM micrograph of bare Fe_3O_4 nanoparticles with size distribution histogram and (c,d) FESEM micrograph of ascorbic acid coated Fe_3O_4 nanoparticles with size distribution histogram

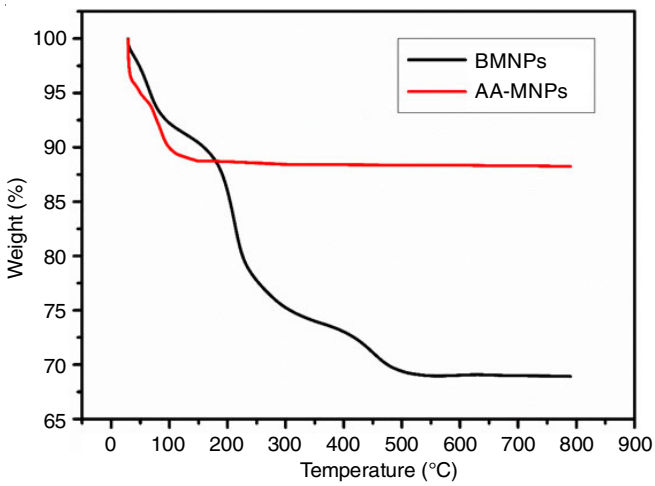

Fig. 5. TGA curve of bare magnetic nanoparticles (BMNPs) and ascorbic acid coated magnetic nanoparticles (AA-MNPs)

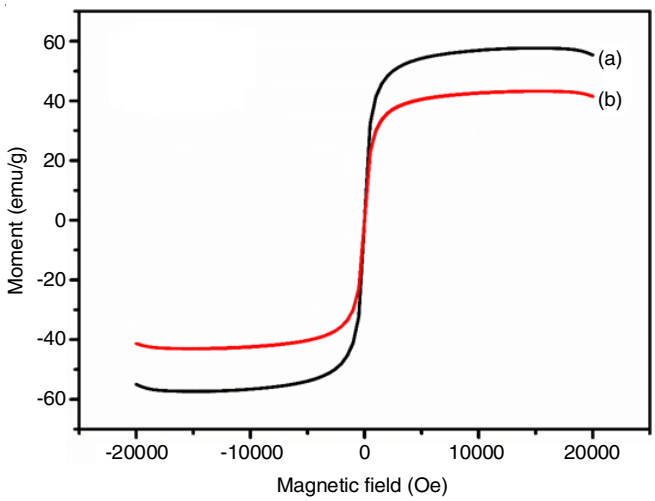

Fig. 6. Magnetic hysteresis loops of (a) Fe_3O_4 nanoparticles and (b) AA-Fe_3O_4 nanoparticles at 300 K

Adsorption studies: The synthesized coated magnetite nanoparticles were used for the removal of SO dye from the aqueous solution. The adsorption of SO dye was investigated by using AA-Fe_3O_4 MNPs as an adsorbent by changing the parameters affecting adsorption capacity such as the quantity of adsorbent, pH, initial concentration of SO dye, contact time and temperature.

Effect of adsorbent amount: The amount of adsorbent is an important parameter in determining the maximum potential for adsorption of dye on its surface. AA-Fe_3O_4 MNPs as an adsorbent showed best result for elimination of SO dye from aqueous solution when it was taken in amount of 5 mg to 30 mg at optimal pH with fixed dye concentrations and fixed contact duration (Fig. 7). The adsorption findings were analyzed and it was concluded that the efficacy of removal for SO dye by AA-Fe_3O_4 was increased up to 97.08% with increase in the amount of adsorbent *i.e.* AA-Fe_3O_4 NPs, which could have been possibly due to the availability of extra active sites, which speed up the adsorption of SO dye molecules on the surface of the AA-Fe_3O_4 NPs [18].

Effect of initial dye concentration: Keeping the amount of adsorbent fixed, under equilibrium conditions, the effect of change in dye concentrations in the range of 10-50 ppm was

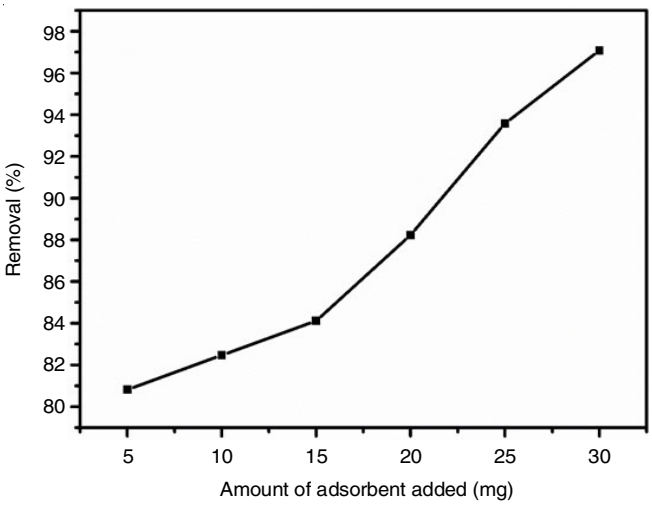

Fig. 7. Effect of adsorbent dose on the removal efficiency of safranin O dye

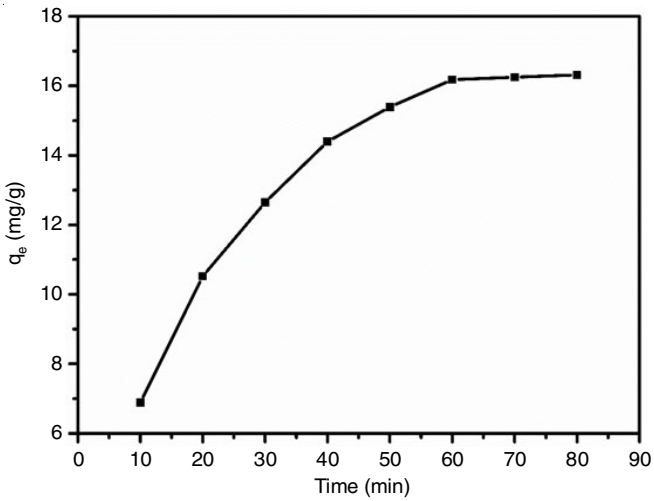

Fig. 9. Adsorption efficiency of AA-Fe_3O_4 nanoparticles for safranin O dye removal at different contact times

investigated on dye adsorption capability on AA-Fe_3O_4 NPs giving expected results. A profile for SO dye adsorption was analyzed with its different initial concentration (Fig. 8), where the adsorption capacity was observed to be decreased as the SO dye concentration was increased stepwise from 10 to 50 ppm. This observation can be explained on the basis of fact that the number of active functional sites of adsorbent are blocked with increase in concentration keeping fixed amount of adsorbent. Therefore, it is assumed that the surface could become saturated with respect to dye. As a result, low concentration of dye may result in improved adsorption process.

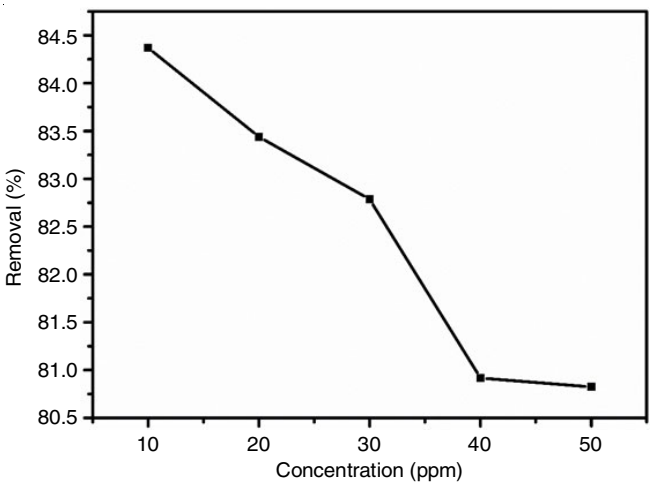

Fig. 8. Effect of initial dye concentration on the removal efficiency of safranin O dye

Effect of contact time: Fig. 9 depicts the influence of contact time on SO dye adsorption at different time intervals (10-80 min) by keeping other parameters fixed such as SO dye concentration (50 ppm) and AA-Fe_3O_4 NPs amount (30 mg). Initially, SO dye adsorption increases with time, but after 60 min, there is no further increase in SO dye adsorption, indicating that 60 min is the equilibrium time. Initially, numerous empty sites increased the adsorption because of the difference in concentration gradient among the adsorbate and the adsorbent. Also, the SO dye molecules clumped together with increase in duration of adsorption process, preventing its adsorption on the surface of adsorbent [24].

pH effect: These findings revealed that the electrostatic attraction played an important role in SO dye adsorption onto AA-Fe_3O_4 NPs. The pH has a significant impact on the adsorption of safranin dye from aqueous solutions. A 0.1 M NaOH and 0.1 M HCl were utilized to alter the pH of SO dye solutions. At different pH values (pH = 3-7), 30 mg of AA-Fe_3O_4 NPs were added to SO dye solution (50 ppm). The rise in pH resulted in an increase in adsorption uptake of SO dye. With increasing pH levels, the adsorption capability of ascorbic acid coated superparamagnetic iron oxide nanoparticles (SPIONs) increases (Fig. 10). This data indicated that the optimal pH for SO dye adsorption is 7. Electrostatic attraction was found to be crucial in the safranin adsorption mechanism on AA-Fe_3O_4 NPs, according to these findings.

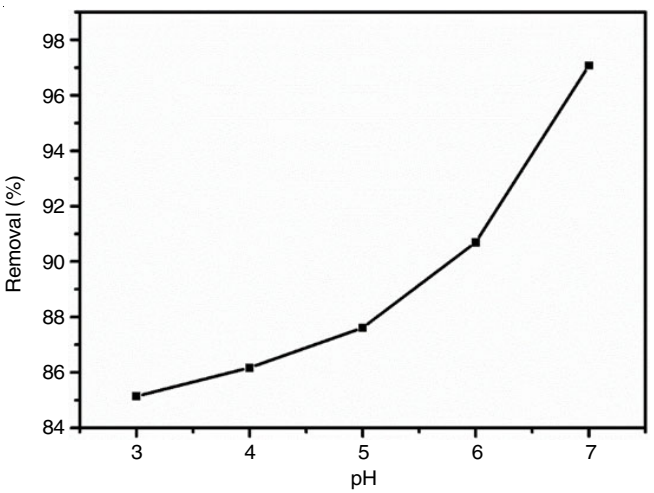

Fig. 10. Effect of pH on safranin O dye removal by AA-Fe_3O_4 nanoparticles

Thermodynamics studies: Thermodynamic study reflected that the adsorption method for removal of SO dye on the surface of functionalized MNPs was spontaneous [25,26]. The effect of temperature on the adsorption of 50 ppm SO dye

on AA-Fe_3O_4 NPs was examined at various temperatures. The experimental data exhibited that as the temperature of the solution increases, the removal efficiency of dye increased as well. This is due to the fact that as temperature increased, the kinetic motion of dye and adsorbent molecules increased, resulting in the better adsorption. On the basis of experimental results, the equilibrium constant (K_c) of the adsorption study was calculated using eqn. 4:

$$K_c = \frac{q_e}{C_e} \quad (4)$$

where q_e is the amount of dye adsorbed onto the surface of AA-Fe_3O_4 NPs at equilibrium (mg/g) and C_e is the equilibrium concentration of the SO dye in solution (ppm) [27]. The following equations (eqns. 5 and 6) were used to calculate thermodynamic parameters such as free energy change (ΔG°), enthalpy change (ΔH°) and entropy change (ΔS°):

$$\Delta G^\circ = -RT \ln K_c \quad (5)$$

$$\ln K_c = \frac{-\Delta H^\circ}{RT} + \frac{\Delta S^\circ}{R} \quad (6)$$

where R represented the universal gas constant (R = 8.314 J/mol K); T represented the absolute temperature (K) and K_c represented the equilibrium constant [28]. The slope and intercept of the plot between ln K_c *vs.* 1/T were used to determine the values of ΔH° and ΔS° (Table-1). The spontaneous nature of adsorption process was reflected by negative value of ΔG° (Table-1). Similarly, the exothermic nature of adsorption of dye on surface of AA-Fe_3O_4 NPs was established by negative values of ΔH°. An increase in degree of randomness at the solid-liquid interface was confirmed by the positive value of ΔS°. Thus, the adsorption of SO dye on surface of AA-Fe_3O_4 was found to be spontaneous and exothermic.

TABLE-1
THERMODYNAMICS PARAMETERS OF SAFRANIN O DYE ADSORPTION ON AA-Fe_3O_4 NANOPARTICLES AT DIFFERENT TEMPERATURES

Temp. (K)	ΔG° (KJ/mol)	ΔH° (KJ/mol K)	ΔS° (J/K mol)
298	-5.958	-40.424	155.173
308	-7.296		
318	-9.066		

Kinetic studies: For the adsorption study, kinetics is very important since it led to determine the rate at which a particular dye can be eliminated from an aqueous solution as well as to get more information about the adsorption mechanism. The pseudo 1st order and pseudo 2nd order models were used to fit the experimentally obtained kinetic data in order to better understand the process of SO dye adsorption onto the surface of AA-Fe_3O_4 nanoparticles.

Lagergren's equation, often known as the pseudo 1st order rate equation, is given by:

$$\log(q_e - q_t) = \log q_e - \frac{k_1 t}{2.303} \quad (7)$$

where q_e is the AA-Fe_3O_4 NPs equilibrium adsorption capacity, q_t represents the AA-Fe_3O_4 NPs adsorption capacity at time t and k_1 denotes the pseudo 1st order rate constant [29]. The pseudo 2nd order model is represented by eqn. 8 as follows:

$$\frac{t}{q_t} = \frac{1}{k_2 q_e^2} + \frac{t}{q_e} \quad (8)$$

where k_2 is the pseudo 2nd order kinetic model's rate constant [30]. Table-2 showed the coefficient of determination (R^2) values for both kinetic models indicating that the pseudo 2nd order model equation can better relate the adsorption rate of SO dye on nanoparticles than the pseudo 1st order kinetic model equation (Fig. 11). The best match to the pseudo 2nd order kinetics indicates that adsorption process is of the chemisorption type.

TABLE-2
KINETIC PARAMETERS FOR THE SAFRANIN O DYE ADSORPTION ON AA-Fe_3O_4 NANOPARTICLES

Pseudo 1st order kinetic model			Pseudo 2nd order kinetic model		
R^2	k_1 (min^{-1})	q_e (mg/g)	R^2	k_2 (g mg^{-1} min^{-1})	q_e (mg/g)
0.985	0.060	18.866	0.999	0.00198	22.371

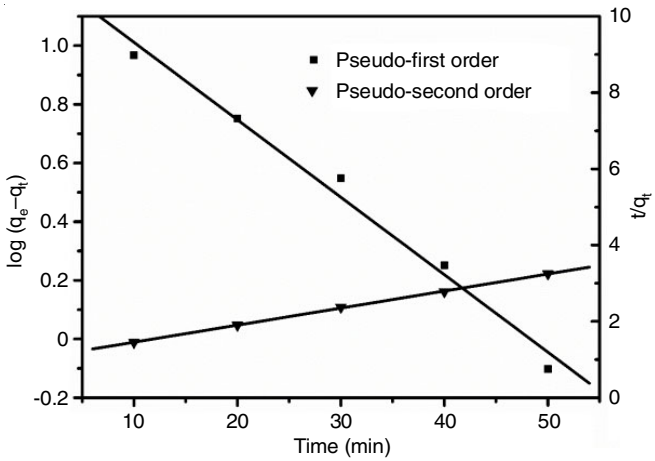

Fig. 11. Pseudo 1st order kinetic plot and pseudo 2nd order kinetic plot for adsorption of safranin O dye on AA-Fe_3O_4 nanoparticles

Adsorption isotherm study: Several isotherm models, like Langmuir, Freundlich and Temkin, have been used to characterize the equilibrium properties of the adsorption in order to optimize the design of an adsorption system for SO dye removal [31]. Fig. 12 illustrates the graphs obtained from the Langmuir, Freundlich and Temkin isotherm models. The Langmuir isotherm model is founded on the idea of adsorbent surface homogeneity, which states that all adsorption sites have the same energy and are identical. The AA-Fe_3O_4 nanoparticles and dye molecule adsorption process should have the same adsorption activation energy and result in the estab-lishment of a monolayer on the AA-Fe_3O_4 nanoparticles surface. The linear form of the Langmuir equation is as follows:

$$\frac{C_e}{q_e} = \frac{1}{q_m K_L} + \frac{C_e}{q_m} \quad (9)$$

where the amount of adsorbed SO dye on the adsorbent at equilibrium (mg/g), the equilibrium concentration of dye solution (mg/L), the Langmuir constant (L/g) and the maximum

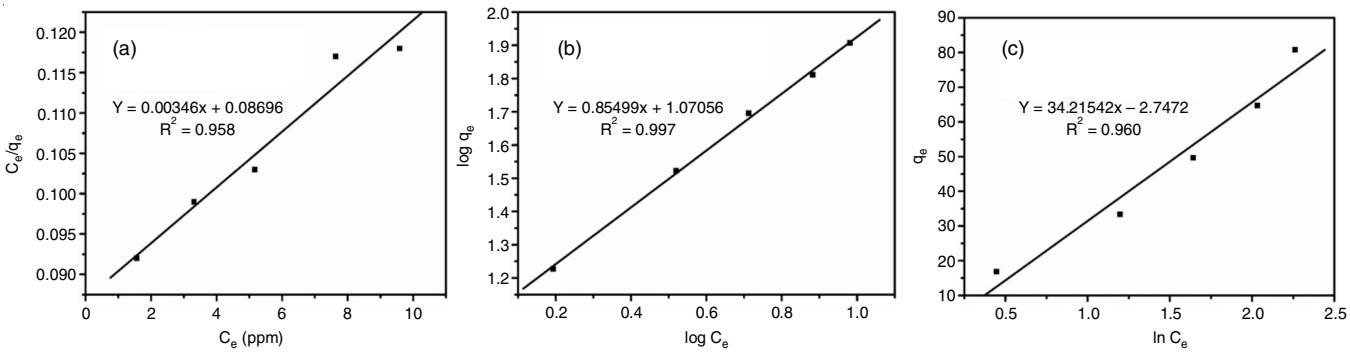

Fig. 12. (a) Langmuir isotherm model, (b) Freundlich isotherm model and (c) Temkin isotherm model

TABLE-3
ISOTHERM PARAMETERS CALCULATED FROM DIFFERENT ISOTHERM MODEL FOR ADSORPTION OF SAFRANIN O DYE ON AA-Fe_3O_4 NANOPARTICLES

Langmuir model			Freundlich model			Temkin model		
R^2	q_m	K_L	R^2	K_F	1/n	R^2	k_1	k_2
0.958	289.01	0.0397	0.997	11.764	0.8549	0.960	34.2154	0.9228

adsorption capacity (mg/g) are represented by q_e, C_e, K_L and q_m, respectively [32]. The Langmuir constant is related to the adsorption free energy. The slope and intercept of the linear plot of C_e *vs*. C_e/q_e were used to compute the q_m value and constant K_L (Fig. 12b).

The assumption in Freundlich model was that adsorption was found to be heterogeneous and multilayer. The Freundlich equation has the following linear form:

$$\log q_e = \log K_F + \frac{1}{n}\log C_e \quad (10)$$

where, K_F and 1/n represents the features of Freundlich constants, K_F denotes the adsorption potential of the adsorbent and 1/n denotes the adsorption intensity [33]. According to the experimental data, linear plot of log q_e *versus* log C_e was used to calculated the values for K_F and 1/n (Fig. 12c).

The reduced sorption heat is assumed to be linear in Temkin model and the binding energy distribution is uniform. It takes indirect adsorbate-adsorbent interactions into account and predicts a linear decrease in adsorption heat for all molecules inside the layer as a result of these interactions. The Temkin relationship can be expressed in linear form as follows:

$$q_e = k_1 \ln k_2 + k_1 \ln C_e \quad (11)$$

where, k_1 (RT/b) is the heat of adsorption, k_2 is the equilibrium binding constant in L/mg and b is the Temkin constant [34]. From linear plot of q_e *versus* ln C_e, the values of k_1 and k_2 are calculated.

The calculated parameters of the isotherm models are shown in Table-3. The Freundlich adsorption model has a coefficient of determination (R^2) of 0.999, which was greater than the R^2 values for the Langmuir and Temkin adsorption models. As a consequence, the Freundlich model better described SO dye adsorption, implying multilayer and heterogeneous adsorption on surface of AA-Fe_3O_4 NPs.

Comparative studies: Table-4 provides a summary of the highest percentage removal that was employed in this research as well as other adsorbents that were found to be effective in the removal of safranin O dye. It can be seen clearly from the table that other reported adsorbent was less efficient for removing SO dye in comparison of ascorbic acid coated nanoparticles. As a result, AA-Fe_3O_4 nanoparticles have been identified as a potential adsorbent tool in the process of the removing safranin O dye from aqueous solution.

TABLE-4
COMPARING THE PERCENTAGE REMOVAL OF SAFRANIN O DYE BY THE ADSORBENT USED IN THIS STUDY WITH OTHER REPORTED ADSORBENTS

Adsorbent	Removal (%)	Ref.
Citrus reticulata peels	84.75	[10]
Pineapple peels	43.30	[11]
Lignin-g-polyacrylic acid nanoparticles	83.66	[12]
Mesoporous silica MCM-41	91.70	[13]
Coal fly ash	86.50	[14]
Copper oxide nanoparticles synthesized from *Punica granatum* leaf extract	90.45	[15]
Activated carbon prepared from tamarind seeds	55.00	[6]
Ascorbic acid coated MNPs	97.08	This study

Conclusion

Chemical co-precipitation method was used to prepare ascorbic acid coated iron oxide magnetite nanoparticles, which were then characterized by FTIR, FESEM, XRD, TGA and VSM techniques. The major goal of this work was to see how effective these synthesized nanoparticles for removing cationic safranin O (SO) dye from aqueous solution. Numerous parameters like contact time, adsorbent dosage, pH of the solution, initial dye concentration and temperature were all examined as the factors impacting SO dye uptake by AA-Fe_3O_4 nanoparticles. The elimination efficiency of SO dyes was found to be more than 97% at the optimum conditions. Kinetics, isotherm and thermodynamic studies helped to understand the mechanism of SO dye adsorption onto AA-Fe_3O_4 nanoparticles. Thermodynamic coefficients confirmed the exothermic and spontaneous nature of the adsorption process. The Freundlich

isotherm model was found to be the best suited for reflecting the heterogeneous multilayer adsorption on the surface of coated nanoparticles based on the experimental data. The kinetics data analysis revealed that the SO dye adsorption on the surface of AA-Fe_3O_4 nanoparticles was pseudo 2nd order and chemical adsorption in nature. To summarize, AA-Fe_3O_4 nanoparticles were found the potential to remove harmful SO dyes from contaminated wastewater.

ACKNOWLEDGEMENTS

The authors are grateful to Kurukshetra University, Kurukshetra, India for providing the research facilities. One of the authors (Keerti Rani) appreciatively acknowledges to UGC, New Delhi, India, for providing financial support in the form of a Senior Research Fellowship (Award no. NOV2017-114450).

CONFLICT OF INTEREST

The authors declare that there is no conflict of interests regarding the publication of this article.

REFERENCES

1. M.E. Mahmoud, M.A. Khalifa, N.M. El-Mallah, H.M. Hassouba and G.M. Nabil, *Int. J. Environ. Sci. Technol.*, **19**, 141 (2022); https://doi.org/10.1007/s13762-021-03153-0
2. M. Fayazi, D. Afzali, M.A. Taher, A. Mostafavi and V.K. Gupta, *J. Mol. Liq.*, **212**, 675 (2015); https://doi.org/10.1016/j.molliq.2015.09.045
3. R.A. Mansour, A. El Shahawy, A. Attia and M.S. Beheary, *Int. J. Chem. Eng.*, **2020**, 1 (2020); https://doi.org/10.1155/2020/8053828
4. M. Ghaedi, S. Haghdoust, S.N. Kokhdan, A. Mihandoost, R. Sahraie and A. Daneshfar, *Spectrosc. Lett.*, **45**, 500 (2012); https://doi.org/10.1080/00387010.2011.641058
5. Z.M. Senol, U.D. Gül and S. Simsek, *Biomass Convers. Biorefinery*, **12**, 4127 (2021); https://doi.org/10.1007/s13399-020-01216-9
6. V.K. Gupta, R. Jain, A. Mittal, M. Mathur and S. Sikarwar, *J. Colloid Interf. Sci.*, **309**, 464 (2007); https://doi.org/10.1016/j.jcis.2006.12.010
7. H. Tavakkoli and F. Hamedi, *Res. Chem. Intermed.*, **42**, 3005 (2016); https://doi.org/10.1007/s11164-015-2194-z
8. A.M. Ghaedi, M. Ghaedi and P. Karami, *Spectrochim. Acta A Mol. Biomol. Spectrosc.*, **138**, 789 (2015); https://doi.org/10.1016/j.saa.2014.11.019
9. P. Li, W. Xiao, P. Chevallier, D. Biswas, X. Ottenwaelder, M.A. Fortin and J.K. Oh, *ChemistrySelect*, **1**, 4087 (2016); https://doi.org/10.1002/slct.201601035
10. E.F.D. Januário, T.B. Vidovix, L.A. Araújo, L. Bergamasco Beltran, R. Bergamasco and A.M.S. Vieira, *Environ. Technol.*, **43**, 4315 (2022); https://doi.org/10.1080/09593330.2021.1946601
11. M.M.A., *Int. J. Environ. Monit. Anal.*, **2**, 128 (2014); https://doi.org/10.11648/j.ijema.20140203.11
12. J. Azimvand, K. Didehban and S.A. Mirshokraie, *Adsorpt. Sci. Technol.*, **36**, 1422 (2018); https://doi.org/10.1177/0263617418777836
13. S. Kaur, S. Rani, R.K. Mahajan, M. Asif and V.K. Gupta, *J. Ind. Eng. Chem.*, **22**, 19 (2015); https://doi.org/10.1016/j.jiec.2014.06.019
14. A. Abbaz, S. Arris, G. Viscusi, A. Ayat, H. Aissaoui and Y. Boumezough, *Gels*, **9**, 916 (2023); https://doi.org/10.3390/gels9110916
15. T.B. Vidovix, H.B. Quesada, R. Bergamasco, M.F. Vieira and A.M.S. Vieira, *Environ. Technol.*, **43**, 3047 (2022); https://doi.org/10.1080/09593330.2021.1914180
16. J. Singh, A. Jangra, J. Kumar, K. Rani and R. Kumar, *Rasayan J. Chem.*, **13**, 105 (2020); https://doi.org/10.31788/RJC.2020.1315382
17. Z. Hamami and V. Javanbakht, *Ceram. Int.*, **47**, 24170 (2021); https://doi.org/10.1016/j.ceramint.2021.05.128
18. B. Priyadarshini, T. Patra and T.R. Sahoo, *J. Magnes. Alloys*, **9**, 478 (2021); https://doi.org/10.1016/j.jma.2020.09.004
19. M.H. Kahsay, *Appl. Water Sci.*, **11**, 45 (2021); https://doi.org/10.1007/s13201-021-01373-w
20. R. Nodehi, H. Shayesteh and A. Rahbar-Kelishami, *Int. J. Environ. Sci. Technol.*, **19**, 2899 (2022); https://doi.org/10.1007/s13762-021-03399-8
21. H. Tavakkoli and M. Yazdanbakhsh, *Microporous Mesopor. Mater.*, **176**, 86 (2013); https://doi.org/10.1016/j.micromeso.2013.03.043
22. N.A. Merino, B.P. Barbero, P. Ruiz and L.E. Cadús, *J. Catal.*, **240**, 245 (2006); https://doi.org/10.1016/j.jcat.2006.03.020
23. I.M. Lourenço, M.T. Pelegrino, J.C. Pieretti, G.P. Andrade, G. Cerchiaro and A.B. Seabra, *J. Phys. Conf. Ser.*, **1323**, 012015 (2019); https://doi.org/10.1088/1742-6596/1323/1/012015
24. V.K. Gupta, B. Gupta, A. Rastogi, S. Agarwal and A.A. Nayak, *J. Hazard. Mater.*, **186**, 891 (2011); https://doi.org/10.1016/j.jhazmat.2010.11.091
25. K.Y.A. Lin and W. Lee, *Appl. Surf. Sci.*, **361**, 114 (2016); https://doi.org/10.1016/j.apsusc.2015.11.108
26. M. Ghaedi, A.G. Nasab, S. Khodadoust, M. Rajabi and S. Azizian, *J. Ind. Eng. Chem.*, **20**, 2317 (2014); https://doi.org/10.1016/j.jiec.2013.10.007
27. F. Zhang, X. Tang, Y. Huang, A.A. Keller and J. Lan, *Water Res.*, **150**, 442 (2019); https://doi.org/10.1016/j.watres.2018.11.057
28. J. Georgin, B. da Silva Marques, J. da Silveira Salla, E.L. Foletto, D. Allasia and G.L. Dotto, *Environ. Sci. Pollut. Res. Int.*, **25**, 6429 (2018); https://doi.org/10.1007/s11356-017-0975-1
29. S. Pai, S.M. Kini, M.K. Narasimhan, A. Pugazhendhi and R. Selvaraj, *Surf. Interfaces*, **23**, 100947 (2021); https://doi.org/10.1016/j.surfin.2021.100947
30. M. Naghizade Asl, N.M. Mahmodi, P. Teymouri, B. Shahmoradi, R. Rezaee and A. Maleki, *Desalination Water Treat.*, **57**, 25278 (2016); https://doi.org/10.1080/19443994.2016.1151832
31. M. Ghaedi, A. Ansari and R. Sahraei, *Spectrochim. Acta A Mol. Biomol. Spectrosc.*, **114**, 687 (2013); https://doi.org/10.1016/j.saa.2013.04.091
32. S. Agarwal, I. Tyagi, V.K. Gupta, M.H. Dehghani, J. Jaafari, D. Balarak and M. Asif, *J. Mol. Liq.*, **224**, 618 (2016); https://doi.org/10.1016/j.molliq.2016.10.032
33. I. Ali, S. Afshinb, Y. Poureshgh, A. Azari, Y. Rashtbari, A. Feizizadeh, A. Hamzezadeh and M. Fazlzadeh, *Environ. Sci. Pollut. Res. Int.*, **27**, 36732 (2020); https://doi.org/10.1007/s11356-020-09310-1
34. L. Mohammadi, E. Bazrafshan, M. Noroozifar, A. Ansari-Moghaddam, F. Barahuie and D. Balarak, *J. Chem.*, **2017**, 1 (2017); https://doi.org/10.1155/2017/2069519